Rare Metal Materials and Engineering
Volume 51, Issue 9, September 2022
Available online at www.rmme.ac.cn

Science Press

Cite this article as: Fu Xiaoqiang, Kou Shengzhong, Li Xiaocheng, et al. Effect of Er on Amorphous Forming Ability and Mechanical Properties of Zr-based Alloys[J]. Rare Metal Materials and Engineering, 2022, 51(09): 3159-3165.

ARTICLE

Effect of Er on Amorphous Forming Ability and Mechanical Properties of Zr-based Alloys

Fu Xiaoqiang[1,2], Kou Shengzhong[1,2], Li Xiaocheng[1,2], Ding Ruixian[1,2], Li Chunyan[1,2], Li Chunling[3]

[1] School of Materials Science and Engineering, Lanzhou University of Technology, Lanzhou 730050, China; [2] State Key Laboratory of Advanced Processing and Recycling of Nonferrous Metals, Lanzhou University of Technology, Lanzhou 730050, China; [3] School of Mechanical and Electrical Engineering, Lanzhou University of Technology, Lanzhou 730050

Abstract: The $(Zr_{0.55}Cu_{0.3}Al_{0.1}Ni_{0.05})_{100-x}Er_x$ (x=0, 0.5, 1, 2, 3, 4, 5) Zr-based bulk alloy with diameter of 3 mm was prepared by water-cooled copper crucible smelting and copper mold suction casting using zirconium sponge as raw material. By comparing the microstructure and mechanical properties of sponge Zr-based alloy with different Er contents, the influence of Er on the amorphous forming ability, thermal stability, and mechanical properties of Zr-based bulk alloy was studied. Results show that when the zirconium sponge is used as the raw material, the amorphous formation ability and mechanical properties of sponge Zr-based alloy are obviously reduced. The sponge Zr-based amorphous alloy cannot be prepared when x=0. After adding Er element, the amorphous forming ability and mechanical properties of the sponge Zr-based alloy with the amorphous structure are improved obviously. The optimal mechanical properties of the sponge Zr-based alloy are achieved when x=2: the compressive strength σ_{bc} is 2142.5 MPa and the plastic strain ε_p is 10.01% at room temperature. Compared with the amorphous $(Zr_{0.55}Cu_{0.3}Al_{0.1}Ni_{0.05})_{98}Er_2$ alloy with the diameter of 3 mm prepared from high-purity Zr, the compressive strength and plasticity at room temperature of the sponge Zr-based alloy recovers by 97.63% and 69.95%, respectively. The Er addition is beneficial to improve the amorphous forming ability and mechanical properties of sponge Zr-based alloy, which also provides a new approach for low-cost preparation of Zr-based amorphous alloy.

Key words: zirconium sponge; amorphous alloy; Er element; amorphous forming ability; mechanical properties

The bulk metallic glass has been widely used in the engineering field due to its excellent properties, such as high fracture strength, high elastic limit, and good corrosion resistance[1-6]. Compared with other bulk metal glasses, Zr-based bulk metallic glass has better glass transformation ability and mechanical properties, such as corrosion resistance and wear resistance[7,8]. However, the requirement for high-purity raw material and high preparation cost restrict the application of Zr-based bulk metallic glass. The numerous impurities in the industrial raw materials are detrimental to the properties of amorphous alloys. Particularly, the bulk metallic glass is sensitive to oxygen, which leads to heterogeneous nucleation, resulting in the formation of metastable quasicrystal structure and the reduction in the amorphous forming ability[9-11]. It is proved that the addition of alloying and rare earth elements can increase the glass transformation ability of alloy. Zhang et al[12] prepared the large metallic glass by die-casting method with zirconium sponge as raw material and the addition of Y element. Ma[13] and Liang[14] et al found that the amorphous forming ability of Zr-based amorphous alloys can be improved by adding an appropriate amount of rare earth elements, such as Y and Gd. Shi et al[15] found that the addition of Ti element can significantly improve the amorphous forming ability, thermal stability, and mechanical properties of $Zr_{65}Cu_{20}Al_{10}Fe_5$ amorphous alloy. Niu et al[16] added rare earth Er element into the Al-Ni-Y amorphous alloy and found that Er can improve the amorphous forming ability and thermal stability of the amorphous alloy. Liu et al[17] studied the influence of alloying elements addition into ultralow-purity raw materials and found that the alloying

Received date: September 26, 2021
Foundation item: National Natural Science Foundation of China (51971103, 51861021); Key R&D Program of Gansu Province (20YF8GA052)
Corresponding author: Kou Shengzhong, Ph. D., Professor, School of Materials Science and Engineering, Lanzhou University of Technology, Lanzhou 730050, P. R. China, E-mail: kousz@lut.cn

elements can react with oxygen to form oxides, therefore playing a purification role by reducing the reactions with heterogeneous nucleation particles. However, few reports discuss the Er effect on the amorphous forming ability and mechanical properties of Zr-based alloy prepared by zirconium sponge. Li et al[18] prepared $Zr_{63.36}Cu_{14.52}Ni_{10.12}Al_{10}$ amorphous alloy with high-purity Zr as raw material and found that the amorphous forming ability, mechanical properties, and thermal stability are improved after adding rare earth Er element.

In this research, zirconium sponge was used as raw material to prepare $(Zr_{0.55}Cu_{0.3}Al_{0.1}Ni_{0.05})_{100-x}Er_x$ (x=0, 0.5, 1, 2, 3, 4, 5) alloy by the water-cooled copper crucible melting and copper mold suction casting methods. Compared with the amorphous $(Zr_{0.55}Cu_{0.3}Al_{0.1}Ni_{0.05})_{98}Er_2$ alloy prepared from high-purity Zr, the influence of Er addition on the amorphous forming ability, thermal stability, and mechanical properties was investigated.

1 Experiment

The raw materials were Zr (high-purity Zr of 99.95% purity, zirconium sponge of 99% purity), Cu (99.95% purity), Ni (99.98% purity), Al (99.99% purity), and Er (99.99% purity). The sponge Zr-based $(Zr_{0.55}Cu_{0.3}Al_{0.1}Ni_{0.5})_{100-x}Er_x$ (x=0, 0.5, 1, 2, 3, 4, 5) alloy and high-purity Zr-based $(Zr_{0.55}Cu_{0.3}Al_{0.1}Ni_{0.5})_{98}Er_2$ alloy were designed and prepared. The total mass of each alloy specimen was 80 g. All materials were immersed in high purity alcohol with ultrasonic cleaning for 15 min and then dried. The water-cooled copper suspension furnace was evacuated to 2×10^{-4} Pa and then filled with high purity argon to 1.0×10^5 Pa. The gas was pretreated repeatedly for 5 times to reduce the oxygen in the system. Then, a water-cooled copper crucible was used for melting under the protection of argon gas, and the uniform mixing of all elements in the alloy ingot was achieved. After the melting, the alloy bars with diameter of 3 mm and length of 70 mm were prepared by copper mold suction casting. The $(Zr_{0.55}Cu_{0.3}Al_{0.1}Ni_{0.5})_{100-x}Er_x$ alloy bars with x=0, 0.5, 1, 2, 3, 4, 5 and the high-purity Zr-based $(Zr_{0.55}Cu_{0.3}Al_{0.1}Ni_{0.5})_{98}Er_2$ alloy bar were denoted as L-0, L-0.5, L-1, L-2, L-3, L-4, L-5, and H-2, respectively. The prepared alloy rod was cut into the specimen with the ratio of height to diameter of 2∶1 by the diamond slicing machine. Then the specimen was polished by sandpaper. The specimens were ultrasonically cleaned by alcohol for 10 min. After drying, the specimens were prepared for structure characterization by X-ray diffraction (XRD) and static compression tests at room temperature. The D8 ADVANCE XRD device was used with Cu target at scan speed of 4°/min and scan angle of 20°~80°. The Wd-100d microcomputer controlled electronic universal testing machine was used for quasi-static compression tests at room temperature with the strain rate of 1×10^{-4} s^{-1}. The Quanta 450FEG field emission scanning electron microscope (SEM) was used to observe the compressive fracture morphologies of alloys at room temperature. The NETZSCH STA-449 F3 differential scanning calorimeter (DSC) was used to detect the characteristic thermodynamic parameters of the amorphous alloy specimens. The nitrogen was introduced to protect the specimens during the experiments, and the heating rate of the specimens was 20 °C/min. The submicrostructure of L-2 specimen was characterized by JEM-1200EX transmission electron microscope (TEM).

2 Results and Discussion

Fig. 1a shows the appearance of molten alloy ingot with Er addition, where the black impurities and oxide skin can be clearly observed. Fig. 1b shows the ingot morphologies after cooling. It can be seen that the ingot surface is smoother without Er addition. With increasing the Er content, the ingot surface becomes dark gray and the oxides are increased.

Fig. 2 shows XRD patterns of L-0, L-0.5, L-1, L-2, H-2, L-3, L-4, and L-5 specimens. It can be seen that L-0 specimen is not amorphous and has obvious crystallization peaks at 2θ=30°~40° and 2θ=60°~70°. The L-0.5, L-1, L-2, H-2, L-3, L-4, and L-5 specimens are all amorphous due to the absence of obvious crystallization peaks in their XRD patterns. This is because Er is combined with oxygen in zirconium sponge, thereby reducing the oxygen content in zirconium sponge, which is beneficial to the purification of raw materials and the amorphous forming ability of the sponge Zr-based alloy. Inoue et al[19] concluded that when the alloy contains at least three elements and the difference in atom radii is more than 12%, the amorphous forming ability can be enhanced. In this research, the atomic radius of the elements in the alloys is as follows: Er (0.176 nm)>Zr (0.162 nm)>Al (0.143 nm)>Cu (0.128 nm)>Ni (0.125 nm)[20]. The difference of atomic radius can increase the random stacking density between atoms, reduce the atom diffusion, and then improve the amorphous forming ability of alloy system. In addition, the enthalpies of Zr-Ni, Zr-Al, Zr-Cu, and Er-Al are −49, −44, −23, and −38

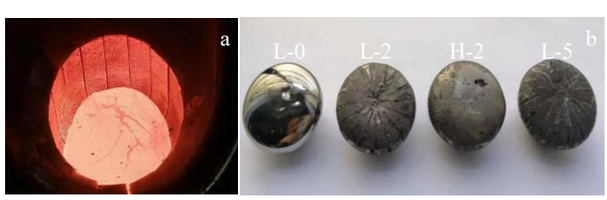

Fig.1 Appearances of melting alloy (a) and alloy ingots (b)

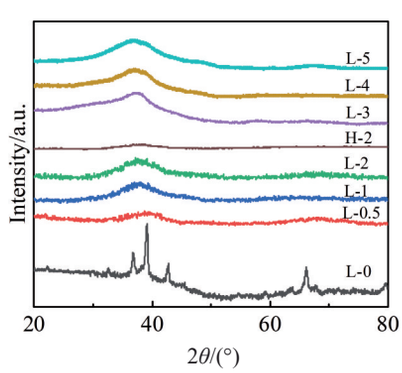

Fig.2 XRD patterns of Zr-based specimens

kJ/mol, respectively, indicating that the appearance of crystal phase can be inhibited, thereby improving the amorphous forming ability. Besides, the Er addition changes the thermodynamic relationship between each alloying element. The amorphous forming ability of amorphous alloy is related to the difference of Gibbs free energy during liquid-solid transformation, as follows[21,22]:

$$\Delta G = \Delta H_m - T\Delta S_m \quad (1)$$

where T is the thermodynamic temperature of the alloy system; H_m and S_m are the melting enthalpy and entropy of the alloy system, respectively. When ΔH_m is low and ΔS_m is high, the low ΔG of alloy system can be obtained. ΔS_m is proportional to the number of components in the alloy system. According to Eq. (1), the Er addition increases ΔS_m while weakens the driving force of melt crystallization, thus improving the amorphous formation ability of the alloy. It can be concluded that the Er addition can significantly improve the amorphous forming ability of sponge Zr-based alloy.

Fig. 3 shows TEM image and selected area electron diffraction (SAED) pattern of L-2 specimen. It can be seen that after adding Er into zirconium sponge, the amorphous forming ability of the sponge Zr-based alloy is significantly improved.

In order to study the effect of Er addition on the thermal stability of sponge Zr-based alloys, the thermal analyses of L-0.5, L-1, L-2, H-2, L-3, L-4, and L-5 specimens were conducted through DSC. Fig. 4 shows the DSC curves of different specimens, and Table 1 shows the experiment data obtained from DSC curves, where T_g is glass transition temperature, T_x is initial crystallization temperature, T_m is melting temperature, and T_l is liquidus temperature. It can be seen that with increasing the temperature, all specimens show a small endothermic reaction caused by the glass transition.

Table 1 also shows the characteristic thermodynamic

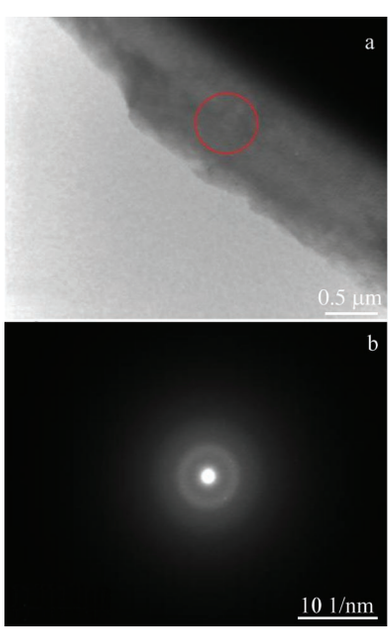

Fig.3 TEM image (a) and SAED pattern (b) of L-2 specimen

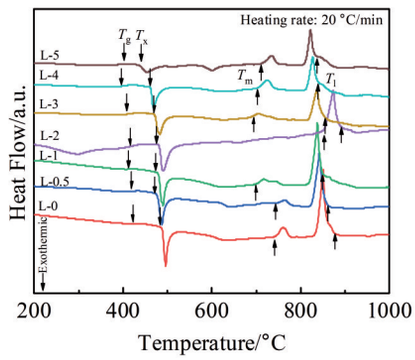

Fig.4 DSC curves of Zr-based specimens

Table 1 Thermodynamic parameters of Zr-based specimens

Specimen	T_g/°C	T_x/°C	T_m/°C	T_l/°C	ΔT_x/°C	T_{rg}	γ
L-0.5	425.3	489.4	745.1	856.5	64.1	0.497	0.382
L-1	408.2	478.1	696.1	852.9	69.9	0.479	0.379
L-2	410.1	480.7	701.2	843.9	70.6	0.486	0.383
H-2	401.7	482.4	725.8	881.9	80.7	0.455	0.376
L-3	416.7	472.1	686.1	847.5	55.4	0.492	0.373
L-4	407.5	463.3	706.2	835.3	55.8	0.488	0.372
L-5	393.3	438.0	715.6	828.7	44.7	0.475	0.358

parameters, such as the width of the supercooled liquid region ($\Delta T_x = T_x - T_g$) of the amorphous alloy. With increasing the Er content, ΔT_x of the amorphous alloy specimen is increased gradually, as shown in Fig. 5. L-2 specimen has the largest ΔT_x of 70.6 °C among the sponge Zr-based $(Zr_{0.55}Cu_{0.3}Al_{0.1}Ni_{0.5})_{100-x}Er_x$ alloys, and its recovery is 87.48% compared with that of H-2 specimen. Because the supercooled liquid phase can inhibit the crystallization nucleation and growth, the smaller the ΔT_x, the smaller the temperature range without crystallization and the worse the thermal stability of the amorphous alloy. On the contrary, the larger the ΔT_x, the higher the interfacial energy between crystalline phase and liquid phase[23] and the better the thermal stability. For amorphous alloy, the reduced glass transition temperature ($T_{rg}=T_g/T_l$) and the parameter $\gamma=T_x/(T_g+T_l)$ are commonly used to evaluate the amorphous forming ability of the amorphous alloy. The larger the T_{rg} or γ, the stronger the amorphous forming ability of the alloy. According to Fig. 5, the amorphous forming ability of sponge Zr-based alloy is decreased firstly, then increased, and finally decreased with increasing the Er content. In addition, the amorphous forming ability of sponge Zr-based alloy is higher than that of high-purity Zr-based alloy when Er content is 2wt%.

In order to investigate the effect of Er addition on mechanical properties of sponge Zr-based alloys, the specimens were subjected to quasi-static room temperature compression tests. The stress-strain curves are shown in Fig. 6. Table 2 shows the corresponding mechanical properties of different amorphous alloys. It can be seen that the sponge Zr-based amorphous alloys with different Er contents all suffer

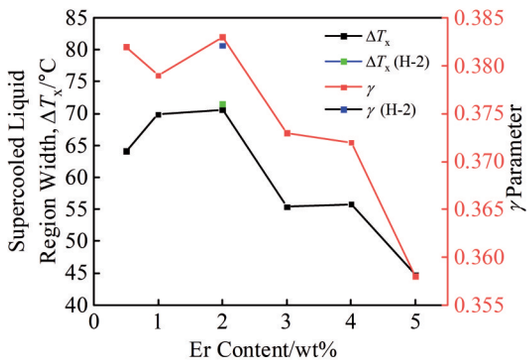

Fig.5 Relationships of ΔT_x and γ parameter with Er content

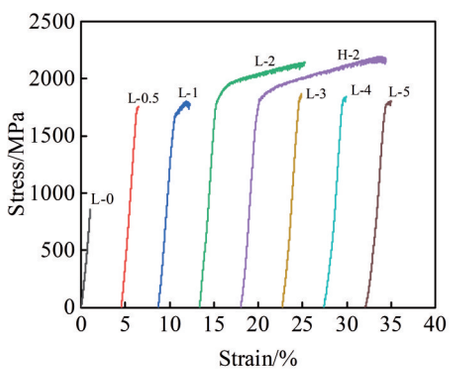

Fig.6 Compressive stress-strain curves of Zr-based specimens at room temperature

the elastic deformation. The L-0 specimen without Er addition shows the brittle fracture after elastic deformation of 1%. L-0.5 and L-1 specimens with a small amount of Er addition present a short period of yield state and they suffer a small amount of plastic deformation after elastic deformation. The L-2 specimen presents obvious yield stage and it suffers large plastic deformation after elastic deformation. No obvious work hardening or sawtooth rheology occurs. Therefore, the Er addition can improve the mechanical properties of sponge Zr-based alloy, indicating that the low-purity raw material can be used for production, which greatly reduces the manufacture cost. However, with further increasing the Er content, the strength and plasticity are decreased significantly. L-2 and H-2 specimens have an obvious serrated rheological phenomenon, during which the rising stress infers the elastic reloading process, while the rapidly decreasing stress infers the rapid softening and shear band expansion. The serrated flow phenomenon reflects the intermittent movement of the shear band. According to the cooperative shear model of the amorphous alloy, the atom clusters in the amorphous alloy can overcome the potential barrier, then transfer to the adjacent zones for deformation, and finally escape from the periodic potential well, resulting in the fracture. The cooperative shear model equation[24] is as follows:

$$\Delta E \propto G\left(\tau - \tau_c\right)^{3/2} \tag{2}$$

$$\tau_c = \pi\varphi_0/4\gamma_c \tag{3}$$

$$\varphi_0 = 8\gamma_c^2 G/\pi^2 \tag{4}$$

where ΔE is the energy barrier difference between two adjacent energy valleys; G is the shear modulus; τ is relaxation time; τ_c is critical relaxation time; φ_0 is the total barrier energy density; γ_c is the yield strain limit with γ_c= 0.0267 for most amorphous alloys[25]. Lots of energy is dissipated by the transference of atom clusters in the compression process, so the accumulated energy in the clusters is relatively low, preventing the fracture caused by the escape of cluster from the potential well. The more obvious the sawtooth rheology, the better the energy dissipation, and the less the fracture possibility. Briefly, the bearing capacity of L-2 specimen is basically equal to that of H-2 specimen. It can be seen from Table 2 that the compressive strength σ_{bc} and fracture strength σ_c of L-0 specimen at room temperature are both 861.1 MPa, and L-0 specimen has no plasticity. The room temperature plastic strain of L-0.5 and L-1 specimens is 0.22% and 1.69%, respectively, indicating that the trace addition of Er can slightly improve the room temperature plasticity. The room temperature plastic stain of L-2 and H-2 specimens is 10.01% and 14.31%, respectively. Compared with that of H-2 specimen, the room temperature plastic strain of L-2 specimen is recovered by 69.95%, indicating that the Er addition can enhance the room temperature plasticity of sponge Zr-based alloy. According to Table 2, the Er addition

Table 2 Mechanical properties of Zr-based specimens

Specimen	Yield strength, σ_s/MPa	Compressive strength, σ_{bc}/MPa	Fracture strength, σ_c/MPa	Plastic strain, ε_p/%
L-0	-	861.1	861.1	-
L-0.5	1730.5	1761.8	1761.8	0.22
L-1	1663.5	1803.3	1779.4	1.69
L-2	1776.7	2142.5	2142.5	10.01
H-2	1813.4	2194.4	2176.0	14.31
L-3	1834.6	1865.7	1865.7	0.25
L-4	1807.2	1842.9	1842.9	0.40
L-5	1765.0	1805.6	1805.6	0.63

can also improve the mechanical properties of sponge Zr-based amorphous alloy. The L-2 specimen has the highest compressive strength σ_{bc} of 2142.5 MPa and the highest fracture strength σ_c of 2142.5 MPa. Compared with those of H-2 specimen, the compressive strength σ_{bc} of L-2 specimen is recovered by 97.63%, and its fracture strength σ_c is recovered by 98.46%.

Fig. 7 shows the shear band morphologies of L-0, L-0.5, L-1, L-2, H-2, L-3, L-4, and L-5 specimens after compression fracture at room temperature. It can be clearly seen that there is no obvious shear band on L-0, L-0.5, and L-3 specimens. The obvious shear zone appears on the L-1 fracture specimen. Compared with L-1 specimen, L-2 specimen has several uniformly distributed shear bands. There are a large number of primary shear bands, secondary shear bands, and capillary shear bands in high-purity Zr-based alloy (H-2 specimen). The existence of these secondary shear bands and capillary shear bands can inhibit the slip of the main shear band to some extent, thus improving the plasticity. The sawtooth rheology in the stress-strain curves indicates the shear band[26,27]. According to Ref. [28], the shear band has more free volume than the matrix does. After the non-uniform plastic deformation, a large number of shear bands are preserved inside the amorphous alloy, so the free volume is increased accordingly. According to the relationship between free volume and plasticity, with increasing the free volume, the viscosity of metallic glass is decreased, the atom mobility becomes better, and the plasticity is enhanced. The relationship between free volume and viscosity is as follows:

$$\eta = \frac{kT}{\nu\Omega}\exp\left(\frac{\gamma v^*}{v_f}\right)\exp\left(\frac{\Delta G_m}{kT}\right) \quad (5)$$

$$x = v_f/(\gamma v^*) \quad (6)$$

where η is the viscosity, k is the Boltzmann constant, Ω is the atomic volume, ν is the Deby frequency, x is the reduced free volume in metallic glass, v_f is the average free volume per atom, v^* is the minimum critical volume required for atomic diffusion in the system, γ is the geometric factor of about 0.1, and ΔG_m is the effective activation energy of atom transference. The atoms are loosely arranged in free volume, resulting in the fact that the atomic bonding is weak and the plastic deformation easily occurs. Therefore, the shear band is easily generated. The larger the free volume, the more the shear bands and multiple shear bands. The multiple shear bands cross each other, thereby restricting each other, which prevents the premature fracture of the amorphous alloy and ultimately leads to enhancement in plasticity[29,30]. The greater the density of the shear bands, the more the shear bands derived from the main shear band, and the greater the room temperature plasticity of the alloys. Therefore, L-0, L-0.5, L-1, and L-3 specimens show little or even no plasticity, and L-2 and H-2 specimens show excellent room temperature plasticity.

Fig. 8 shows the fracture morphologies of L-0, L-0.5, L-1, L-2, H-2, L-3, L-4, and L-5 specimens after compression fracture at room temperature. The L-0 alloy specimen presents lamellar structure, indicating the brittle fracture. Therefore, L-0 specimen has no plasticity. L-0.5 and L-1 specimens show a few uneven veins, indicating the slight plasticity. L-2 specimen has more uneven veins. However, H-2 specimen has dense and uniform veins. Thus, the plasticity of L-2 specimen is worse than that of H-2 specimen. It can be concluded that the denser and the more uniform the veins, the better the

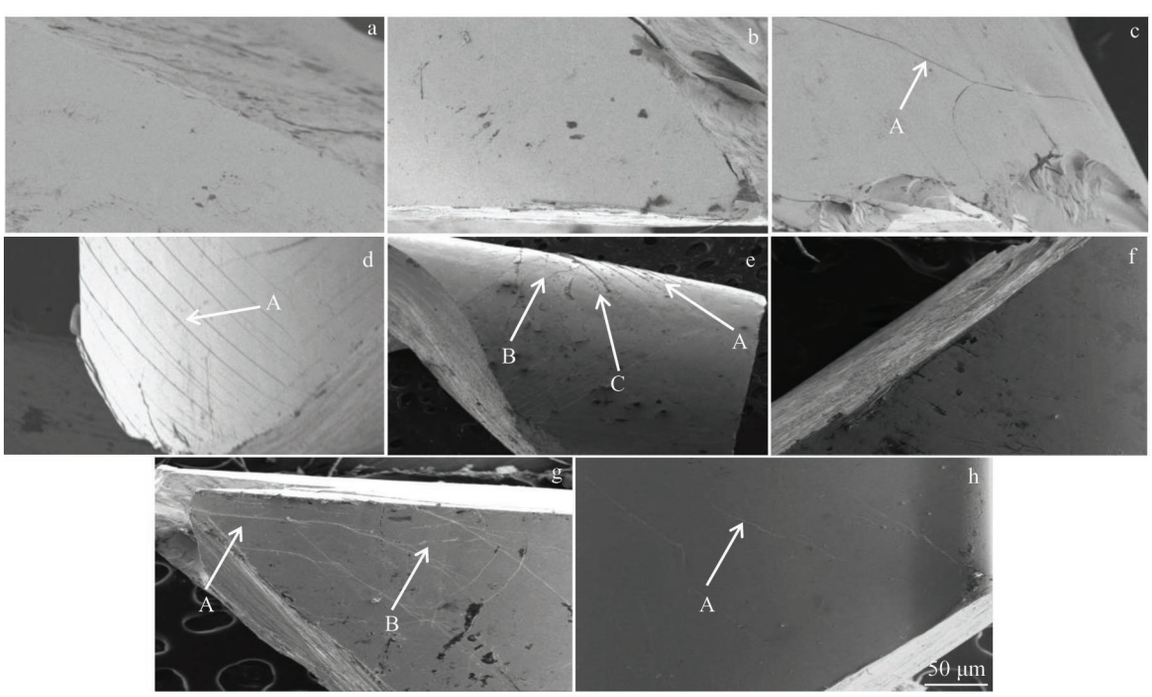

Fig.7 Shear band morphologies of Zr-based specimens after compression fracture at room temperature: (a) L-0, (b) L-0.5, (c) L-1, (d) L-2, (e) H-2, (f) L-3, (g) L-4, and (h) L-5 (A: main shear band; B: secondary shear zone; C: capillary shear zone)

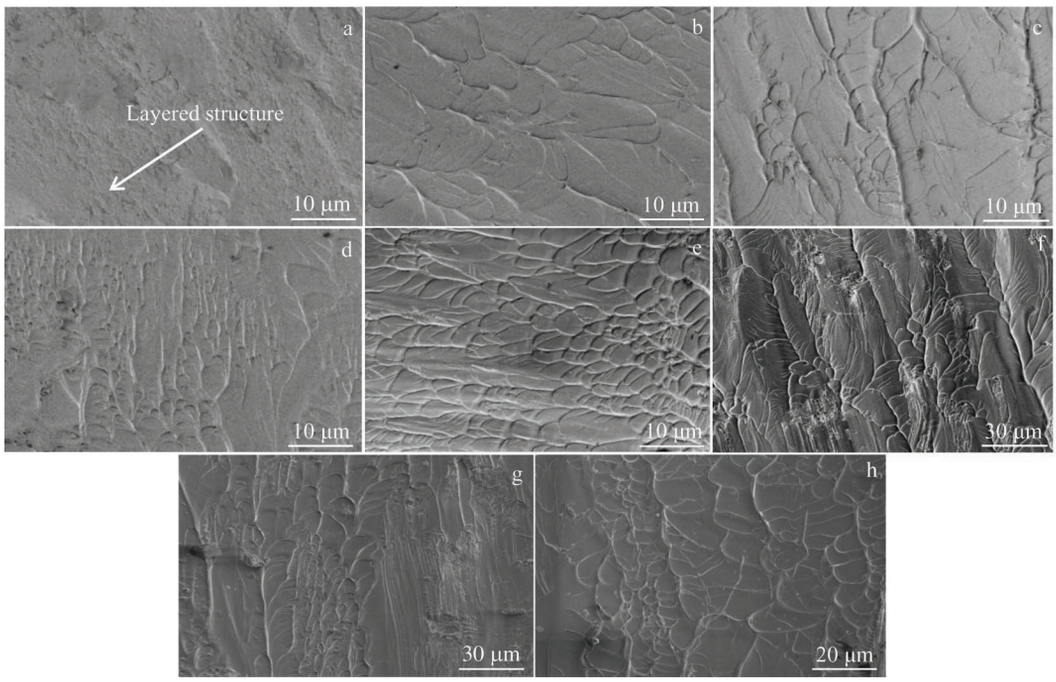

Fig.8 Compression fracture morphologies of Zr-based specimens at room temperature: (a) L-0, (b) L-0. 5, (c) L-1, (d) L-2, (e) H-2, (f) L-3, (g) L-4, and (h) L-5

plasticity of alloys at room temperature.

3 Conclusions

1) The Er addition can effectively purify the zirconium sponge by increasing the atom size difference of alloying elements and raising the entropy of alloy system. Therefore, the amorphous forming ability of sponge Zr-based alloys can be significantly improved. In addition, the optimal amorphous forming ability is achieved with 2wt% Er addition.

2) Er addition can widen the supercooled liquid region and improve the thermal stability of the amorphous zirconium sponge alloys. Compared with that of the high-purity Zr-based $(Zr_{0.55}Cu_{0.3}Al_{0.1}Ni_{0.5})_{98}Er_2$ alloy, the width of the supercooled liquid region of the sponge Zr-based amorphous alloy with 2wt% Er addition is recovered by 87.48%.

3) The Er addition can obviously improve the mechanical properties of the sponge Zr-based amorphous alloys. Compared with those of the high-purity Zr-based $(Zr_{0.55}Cu_{0.3}Al_{0.1}Ni_{0.5})_{98}Er_2$ alloy, the compressive strength, fracture strength, and room temperature plasticity of sponge Zr-based amorphous alloy with 2wt% Er addition are recovered by 97.63%, 98.46%, and 69.95%, respectively.

References

1 Hufnagel T C, Schuh C A, Falk M L. *Acta Materialia*[J], 2016, 109: 375

2 Inoue A, Takeuchi A. *Acta Materialia*[J], 2010, 59(6): 2243

3 Kumar G, Neibecker P, Liu Y H *et al*. *Nature Communications*[J], 2013, 4(1): 536

4 Louzguine-Luzgin D V, Louzguina-Luzgina L V, Churyumov A Y. *Metals*[J], 2013, 3(1): 1

5 Li H X, Lu Z C, Wang S L *et al*. *Progress in Materials Science*[J], 2019, 103: 235

6 Schroers J. *Advanced Materials*[J], 2010, 22(14): 1566

7 Qin C L, Zeng Y Q, Louzguine D V *et al*. *Journal of Alloys and Compounds*[J], 2010, 504: 172

8 Tsai P H, Lee C I, Song S M *et al*. *Coatings*[J], 2020, 10(12): 1212

9 Lu Z P, Bei H, Wu Y *et al*. *Applied Physics Letters*[J], 2008, 92(1): 148

10 Murty B S, Ping D H, Hono K *et al*. *Acta Materialia*[J], 2000, 48(15): 3985

11 Murty B S, Ping D H, Hono K *et al*. *Applied Physics Letters*[J], 2000, 76(1): 55

12 Zhang T, Meng X M, Wang C Y *et al*. *Journal of Alloys and Compounds*[J], 2019, 792: 851

13 Ma Mingzhen, Liang Shunxing, Chen Jun *et al*. *Journal of Yanshan University*[J], 2011, 35(5): 423 (in Chinese)

14 Liang Shunxing, Zong Haitao, Ma Mingzhen *et al*. *Special Casting and Nonferrous Alloys*[J], 2008, 29(S1): 277 (in Chinese)

15 Shi H Q, Zhao W B, Wei X W *et al*. *Journal of Alloys and Compounds*[J], 2020, 815: 152 636

16 Niu Ben, Zhao Qingming, Tian Ye *et al*. *Journal of the Chinese Society of Rare Earth*[J], 2008, 26(4): 450 (in Chinese)

17 Liu Z Q, Yang Y W, Li R *et al*. *Chinese Science Bulletin*[J], 2012, 57(30): 3931

18 Li C Y, Yin J F, Ding J Q *et al*. *Materials Science and Technology*[J], 2018, 34(15): 1887

19 Inoue A. *Acta Materialia*[J], 2000, 48(1): 279
20 Takeuchi A, Inoue A. *Materials Transactions*[J], 2005, 46(12): 2817
21 Lad K N, Raval K G, Pratap A. *Journal of Non-Crystalline Solids* [J], 2004, 334(6): 259
22 Lad K N, Pratap A, Raval K G. *Journal of Materials Science Letters*[J], 2002, 21(18): 1419
23 Ling Z L, Liu W, Zhong M *et al*. *Journal of Thermal Analysis and Calorimetry*[J], 2018, 132(3): 1645
24 Li Chunyan, Yin Jinfeng, Wang Zheng *et al*. *Journal of Materials Engineering*[J], 2018, 46(1): 1 (in Chinese)
25 Wang Weihua. *Progress in Physics*[J], 2013, 33(5): 177 (in Chinese)
26 Yang G N, Chen S Q, Gu J L *et al*. *Philosophical Magazine*[J], 2016, 96(21): 2243
27 Yang G N, Gu J L, Chen S Q *et al*. *Metallurgical and Materials Transactions*[J], 2016, 47(11): 5395
28 Shi Bo, Wang Jinhui, Wei Fuan. *Materials Reports*[J], 2019, 33(7): 146 (in Chinese)
29 Chen L Y, Fu Z D, Zhang G Q *et al*. *Physical Review Letters*[J], 2008, 100(7): 75 501
30 Liu C, Ikeda Y, Maaß R. *Scripta Materialia*[J], 2021, 190: 75

铒元素对锆基合金的非晶形成能力及力学性能的影响

付小强[1,2]，寇生中[1,2]，李晓诚[1,2]，丁瑞鲜[1,2]，李春燕[1,2]，李春玲[3]
(1. 兰州理工大学 材料科学与工程学院，甘肃 兰州 730050)
(2. 兰州理工大学 省部共建有色金属先进加工与再利用国家重点实验室，甘肃 兰州 730050)
(3. 兰州理工大学 机电工程学院，甘肃 兰州 730050)

摘 要：以海绵锆为原料，采用水冷铜坩埚熔炼和铜模吸铸法制备了直径为3 mm、成分为$(Zr_{0.55}Cu_{0.3}Al_{0.1}Ni_{0.05})_{100-x}Er_x$ (x=0，0.5，1，2，3，4，5)的锆基块体合金，通过对比不同铒含量海绵锆基合金的组织结构与性能，研究了铒元素对其非晶形成能力、热稳定性和力学性能的影响。结果表明：以海绵锆为原料时，锆基合金的非晶形成能力和力学性能明显下降。x=0时，无法制备成锆基非晶合金；添加Er元素后，海绵锆基合金的非晶形成能力和力学性能显著提高，具有非晶态结构；x=2时，海绵锆基非晶合金的力学性能最优，抗压强度σ_{bc}为2142.5 MPa，室温下塑性应变ε_p为10.01%。与高纯锆制备的同直径$(Zr_{0.55}Cu_{0.3}Al_{0.1}Ni_{0.05})_{98}Er_2$非晶合金相比，其抗压强度恢复97.63%，室温塑性恢复69.95%。添加铒元素有利于改善和提高海绵锆基合金的非晶形成能力和力学性能，为低成本制备锆基非晶合金提供一种新思路。

关键词：海绵锆；非晶合金；铒元素；非晶成形能力；力学性能

作者简介：付小强，男，1994年生，硕士，兰州理工大学材料科学与工程学院，甘肃 兰州 730050，E-mail：kousz@lut.cn